In vitro leishmanicidal activity of pyrazole-containing polyamine macrocycles which inhibit the Fe-SOD enzyme of *Leishmania infantum* and *Leishmania braziliensis* species

P. NAVARRO[1]*, M. SÁNCHEZ-MORENO[2], C. MARÍN[2], E. GARCÍA-ESPAÑA[3], I. RAMÍREZ-MACÍAS[2], F. OLMO[2], M. J. ROSALES[2], F. GÓMEZ-CONTRERAS[4], M. J. R. YUNTA[4] *and* R. GUTIERREZ-SÁNCHEZ[5]

[1] *Instituto de Química Médica, Centro de Química Orgánica M. Lora-Tamayo, CSIC, E-28006 Madrid, Spain*
[2] *Departamento de Parasitología, Facultad de Ciencias, Universidad de Granada, E-18071 Granada, Spain*
[3] *Departamento de Química Inorgánica, Instituto de Ciencia Molecular, Universidad de Valencia, E-46980 Paterna (Valencia), Spain*
[4] *Departamento de Química Orgánica, Facultad de Química, Universidad Complutense, E-28040 Madrid, Spain*
[5] *Departamento de Estadística. Facultad de Ciencias, Universidad de Granada, E-18071 Granada, Spain*

(*Received 8 October 2013; revised 9 November 2013 and 20 January 2014; accepted 20 January 2014; first published online 17 March 2014*)

SUMMARY

The *in vitro* leishmanicidal activity and cytotoxicity of pyrazole-containing macrocyclic polyamines **1–4** was assayed on *Leishmania infantum* and *Leishmania braziliensis* species. Compounds **1–4** were more active and less toxic than glucantime and both infection rates and ultrastructural alterations confirmed that **1** and **2** were highly leishmanicidal and induced extensive parasite cell damage. Modifications in the excretion products of parasites treated with **1–3** were also consistent with substantial cytoplasm alterations. Compound **2** was highlighted as a potent inhibitor of Fe-SOD in both species, whereas its effect on human CuZn-SOD was poor. Molecular modelling suggested that **2** could deactivate Fe-SOD due to a sterically favoured enhanced ability to interact with the H-bonding net that supports the enzyme`s antioxidant features.

Key words: *Leishmania braziliensis*, *Leishmania infantum*, iron superoxide dismutase, leishmanicidal activity, pyrazole, polyamine macrocycle.

INTRODUCTION

Among the vector-borne diseases caused by protozoa, leishmaniasis is especially widespread, since it is endemic in many countries of Latin America, in the Indian subcontinent, in East Africa and in the Mediterranean Basin (Sundar and Chatterjee, 2006; WHO, 2010). Furthermore, travel to and from endemic areas has contributed to spreading the disease to previously safe countries (Amato *et al*. 2007). Leishmaniasis may be quite diverse, because it is caused by many different parasitic species, transmitted by different vectors and animal reservoirs, and there are different clinical syndromes (Chappuis *et al*. 2007). Among the latter, cutaneous leishmaniasis (CL), which produces ulcers on exposed parts of the body, mucosal leishmaniasis (ML), characterized by non-self-healing destructive ulcerations of the mucosa, and visceral leishmaniasis (VL), presenting with anaemia, systemic infection, bleeding and, if untreated, usually leading to death, are the predominant clinical forms. Although CL is the most common form, ML and VL are the most severe, so we have selected representative species for both of them. *Leishmania braziliensis* is one of the most usual species that cause ML, and is mainly active in Brazil, Colombia, Venezuela and the Andes range (Guerra *et al*. 2011). *Leishmania infantum* is the primary agent responsible for VL in Europe, North Africa and Latin America (Lukes *et al*. 2007).

The preferred treatment strategies against leishmaniasis include pentavalent antimonials and amphotericin B in most regions of the world, although the use of new compounds such as miltefosine or paromomycin for the treatment of ML, and allopurinol or itraconazole for VL, is slowly being introduced, with controversial results. However, adverse effects, relative efficacy and the elevated costs involved encourage the design of new effective drugs. Treatments of ML-affected individuals have to deal with widespread increasing drug resistance and moderate cure rates (Croft *et al*. 2006; Woster, 2007; Palumbo, 2009).

Assuming the need for new drugs against leishmaniasis, different parasite targets have been proposed. One of the most striking characteristics of the *Leishmania* parasites consists of its ability to survive in the presence of reactive oxygen species generated by the macrophages in which they are hosted. Therefore, it is not surprising that the therapeutic

* Corresponding author: Instituto de Química Médica, Centro de Química Orgánica M. Lora-Tamayo, CSIC, E-28006 Madrid, Spain. E-mail: fercon@ucm.es and iqmnt38@iqm.csic.es

doi:10.1017/S0031182014000201

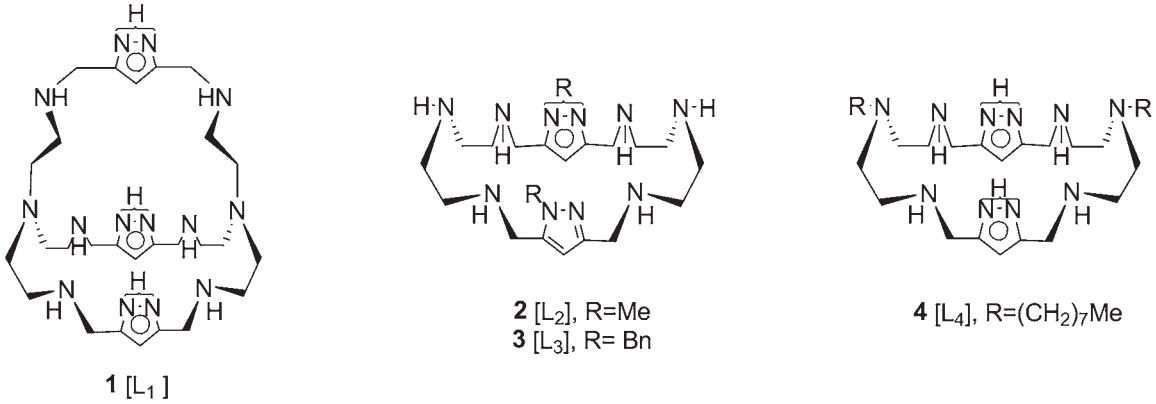

Fig. 1. Pyrazole-containing polyamine macrocycles tested against *Leishmania infantum* and *Leishmania braziliensis* in the present study.

targets most investigated are enzymes involved in antioxidant defence that are either exclusive to the parasite or present significant differences with respect to their homologues in humans (Van Assche *et al*. 2011; Deschacht *et al*. 2012). Within this context, one enzyme that plays an essential role in the struggle of the parasite against oxidative stress is iron superoxide dismutase (Fe-SOD), which is present in all trypanosomatids (Miller, 2004), but not in humans, so that compounds able to selectively inhibit Fe-SOD are potential drugs for the treatment of leishmaniasis (Turrens, 2004).

In search of structures with the ability to interact with the active site of the enzyme, we focused our interest in macrocyclic polyamines containing highly complexing pyrazole units and presenting different protonation degrees at physiological pH (compounds **1–4**, Fig. 1). Macrobicyclic polyamine **1** (Lamarque *et al*. 2001), macrocyclic polyamines **2** and **3** (Arán *et al*. 1999; Kumar *et al*. 2001), with N-methyl- and N-benzyl-substituted pyrazole rings, and macrocyclic analogue **4** (Miranda *et al*. 2004), with bulky octyl groups attached to the amine nitrogens on the side-chains had been previously tested by us against *Trypanosoma cruzi* (Sánchez-Moreno *et al*. 2012*a*). In those assays it was found that compounds **1–3** were more active against the parasite and less toxic against Vero cells than the reference drug benznidazole (BZN), whereas the behaviour of **4** was similar to that of BZN or even worse. When inhibition of SOD enzymes by **1–4** was also tested, it was found that all four compounds selectively inhibited parasitic Fe-SOD in comparison with mammal CuZn-SOD, but the greatest selectivity and inhibitory activity were found with compounds **1** and **2**, with the worst results again being those obtained with the bulky compound **4**. On the basis of these data a potential relationship between the anti-parasitic activity observed and the ability of the compounds to interact with the enzyme was tentatively suggested.

Taking into account the very close structural similarity of the Fe-SOD enzymes in *T. cruzi* and *Leishmania* spp., it was considered of interest to investigate the leishmanicidal activity of **1–4**. In this work, their antiproliferative activity against both *L. infantum* and *L. braziliensis* and non-specific mammalian cytotoxicity were evaluated *in vitro*, and these measures were complemented by infectivity assays on macrophage cells. Furthermore, the treated parasites were submitted to a thorough study of the possible behaviour of the compounds assayed, as follows: (i) alterations caused in the cell ultrastructure of the parasites were recorded using transmission electronic microscopy (TEM); (ii) a ^{1}H-NMR study concerning the nature and percentage of metabolite excretion was performed in order to obtain information on the effect of the polyamine macrocycles on the glycolytic pathway, since it represents the primary source of energy for the parasite; and (iii) inhibition of the parasitic Fe-SOD and human CuZn-SOD enzymes was tested and compared, and the mode of interaction with the enzyme's active site was simulated by molecular modelling.

MATERIALS AND METHODS

Chemistry

3,5-Dimethyl-1*H*-pyrazole, tris-2-(aminoethyl) amine, and 1,5-diamino-3-azapentane were purchased from commercial sources (Sigma-Aldrich) and used without further purification. 1,5-diamino-3-octylazapentane is not commercial and was obtained from 1,5-diamino-3-azapentane (Miranda *et al*. 2004). 1*H*-pyrazole-3,5-dicarbaldehyde and 1-benzyl-1*H*-pyrazole-3,5-dicarbaldehyde were obtained from 3,5-dimethyl-1*H*-pyrazole according to a procedure previously described by the research group of one of the authors (Arán *et al*. 1999). 1-Methyl-1*H*-pyrazole-3,5-dicarbaldehyde was obtained from diethyl 1*H*-pyrazole-3,5-dicarboxylate as described by Kumar *et al*. (2001). The solvents were dried using standard techniques (Perrin *et al*. 1980). All reactions were monitored by thin layer chromatography

https://doi.org/10.1017/S0031182014000201 Published online by Cambridge University Press

(TLC) using DC-Alufolien Silica gel $60PF_{254}$ (Merck; layer thickness, 0·2 mm). The compounds were detected using UV light (254 nm), iodine or phosphomolybdic acid. Melting points were determined using a Reichert-Jung hot-stage microscope and are uncorrected. The ^{1}H- and ^{13}C-NMR spectra were recorded on Varian Inova-300, Varian Inova-400 and Varian Unity-500 spectrometers at room temperature employing CD_3OD, $CDCl_3$ or D_2O as solvents. The chemical shifts were reported in parts per million (ppm) from tetramethylsilane (TMS), but were measured against the solvent signals. All assignments were made on the basis of ^{1}H-^{13}C heteronuclear multiple quantum coherence (gHMQC) and heteronuclear multiple bond coherence (gHMBC) experiments. The electrospray ionization (ESI) mass spectra (MS) were registered on a Hewlett-Packard 1100 MSD spectrometer in the electrospray positive mode. The fast atom bombardment (FAB) MS were obtained on a VG AutoSpec spectrometer using an *m*-nitrobenzyl alcohol matrix. Elemental analyses were performed by the Departamento de Analisis, Centro de Química Orgánica 'Manuel Lora-Tamayo', CSIC, Madrid, Spain. Elemental analysis was used to confirm a purity higher than 95% for all the biologically tested compounds.

*Preparation of the pyrazole-containing bicyclic polyamine **1***

1*H*-Pyrazole-3,5-dicarbaldehyde (Arán *et al*. 1999) (372 mg, 3 mmol), was dissolved in warm methanol (180 mL) and added dropwise under an argon atmosphere to a stirred solution of tris (2-aminoethyl)amine (292 mg, 2 mmol) in methanol (120 mL). After stirring overnight at room temperature, the intermediate Schiff base was reduced *in situ* with solid sodium borohydride (340 mg, 9 mmol) by stepwise addition. After 2 h, a standard work-up of the reaction mixture (Sánchez-Moreno *et al*. 2012*a*) afforded 345 mg (59%) of 1,4,7,8,11,14,17,20,21,24,29,32,33,36-tetradecaazapentacyclo-[12.12.12.^{6,9}.1^{19,22}.1^{31,34}]-hentetraconta-6,9(41),19(40),21,31,34(39)-hexene in the monohydrate form (**1**, melting point (mp) 244–245 °C (lit mp: 245 °C; Lamarque *et al*. 2001), MS (FAB): 569 (M^+ +1).

*Preparation of the pyrazole-containing monocyclic polyamine **2***

A solution of 1-methyl-1*H*-pyrazole-3,5-dicarbaldehyde (Kumar *et al*. 2001) (276 mg, 2 mmol) in MeCN (10 mL) was added, under argon, to a solution of freshly distilled 1,5-diamino-3-azapentane (206 mg, 2 mmol) in the same solvent (20 mL). After stirring overnight at room temperature, the intermediate Schiff base was reduced *in situ* by addition of sodium borohydride (304 mg, 8 mmol) in MeOH (40 mL). After 2 h, a standard work-up of the reaction mixture (Sánchez-Moreno *et al*. 2012*a*) afforded 267 mg (64%) of 13,26-Dimethyl-3,6,9,12,13,16,19,22,25,26-decaazatricyclo-[22.2.1.1^{11,14}]-octacosa-1(27),11,14(28),24-tetraene (**2**, mp 134–135 °C) (lit.: thick oil; Kumar *et al*. 2001), MS (ESI^+, MeOH): 419 (M^+ + 1).

*Preparation of the pyrazole-containing monocyclic polyamine **3***

A solution of 1-benzyl-1*H*-pyrazole-3,5-dicarbaldehyde (Arán *et al*. 1999) (428 mg, 2 mmol) in MeCN (30 mL) was added under argon, to a solution of freshly distilled 1,5-diamino-3-azapentane (204 mg, 2·0 mmol) in the same solvent (30 mL). After stirring overnight at room temperature, the intermediate Schiff base separated as a white solid that was crystallized from EtOH (405 mg, 72%, mp 161–162 °C) (lit. 160–162 °C; Arán *et al*. 1999). A stirred suspension of the above Schiff base (394 mg, 0·7 mM) in EtOH (20 mL) was reduced by stepwise addition of solid sodium borohydride (303 mg, 8·0 mM). After stirring for 2 h at room temperature, a standard work-up of the reaction mixture (Sánchez-Moreno *et al*. 2012*a*) afforded 299 mg (75%) of 13,26-Dibenzyl-3,6,9,12,13,16,19,22,25,26-decaazatricyclo-[22.2.1.1^{11,14}]-octacosa-1(27),11,14(28),24-tetraene (**3**, mp 137–138 °C) (lit. 136–138 °C; Arán *et al*. 1999). MS (FAB): 571 (M^+ + 1).

*Preparation of the pyrazole-containing monocyclic polyamine **4***

1*H*-Pyrazole-3,5-dicarbaldehyde (Arán *et al*. 1999) (248 mg, 2 mmol) was dissolved in hot MeOH (130 mL). This solution was then cooled to room temperature and added dropwise under argon to a stirred solution of 1,5-diamine-3-octyl-3-azapentane (Miranda *et al*. 2004) (431 mg, 2 mM) in MeOH (220 mL). After stirring 12 h at room temperature, the intermediate Schiff base was reduced *in situ* with solid sodium borohydride (454 mg, 12 mmol) by stepwise addition. After 2 h, a standard work-up of the reaction mixture afforded the dihydrated monocyclic polyamine 6,19-Dioctyl-3,6,9,12,13,16,19,22,25,26-decaazatricyclo-[22.2.1.1^{11,14}]-octacosa-1(27),11,14(28),24-tetraene (**4**, 299 mg, 46%), as a colourless syrup (TLC: Rf = 0·54, MeOH 10:1). MS (ESI^+, MeOH): 616 (M^+ +1).

Parasite strain and culture

Leishmania infantum (MCAN/ES/2001/UCM-10) and *L. braziliensis* (MHOM/BR/1975/M2904) were cultured *in vitro* in Medium Trypanosomes Liquid medium (MTL) together with 10% inactive fetal calf serum (FCS) kept in an air atmosphere at 28 °C, in Roux flasks (Corning, USA) with a surface area of

https://doi.org/10.1017/S0031182014000201 Published online by Cambridge University Press

75 cm^2, according to a methodology previously described (González *et al*. 2005).

In vitro *activity assays: extracellular forms*

Promastigote assay. The compounds were dissolved in DMSO (Panreac, Barcelona, Spain) at a concentration of 0·1% and were assayed as non-toxic and without inhibitory effects on parasite growth, as previously described (González *et al*. 2005). The compounds were dissolved in the culture medium at concentrations from 0·1 to 100 μM. The effects of each compound against the promastigote forms and its concentrations were tested at 72 h using a Neubauer haemocytometric chamber. The leishmanicidal effect was expressed as the IC_{50} value, i.e. the concentration required to result in 50% inhibition, calculated by linear regression analysis from the K_c values of the concentrations employed. Values are the means of three separate determinations.

Cell culture and cytotoxicity tests. The macrophage line J774.2 [European collection of cell cultures (ECACC) number 91051511] was derived in 1968 from a tumour in a female BALB/c mouse, and macrophages were grown in minimal essential medium (MEM) plus glutamine (2 mM) and 20% inactive FCS, with a humidified atmosphere of 95% air and 5% CO_2 at 37 °C. The cytotoxicity test on macrophages was performed by flow cytometric analysis according to a method previously described (Marín *et al*. 2011). The percentage of viability was calculated with respect to the control culture. The IC_{50} was calculated using linear regression analysis from the K_c values of the concentrations employed. Values are the means of three separate determinations.

Infectivity assay. J774.2 macrophage cells were grown as described above and seeded at a density of 1×10^4 cells $well^{-1}$ in 24-well microplates (Nunc) with rounded coverslips on the bottom and cultured for 2 days. The cells were then infected *in vitro* with promastigote forms of *L. infantum* or *L. braziliensis* at a ratio of 10 : 1. The drugs (IC_{25} concentrations) were added immediately after infection and incubation was performed for 12 h at 37 °C in 5% CO_2. Non-phagocytosed parasites and drugs were removed by washing, and then the infected cultures were grown for 10 days in fresh medium. Cultures were washed every 48 h and fresh culture medium was added. Drug activity was determined on the basis of both the percentage of infected cells and the number of amastigotes per infected cell in treated and untreated cultures in methanol-fixed and Giemsa-stained preparations. The percentage of infected cells and the mean number of amastigotes per infected cell were determined by analysing more than 200 host cells distributed in randomly chosen microscopic fields. Values are the means of three separate determinations.

In vitro activity assays: intracellular forms. Adherent macrophage cells were infected with promastigotes in the stationary growth phase of *Leishmania* spp. at a ratio of 10 : 1 and maintained for 24 h at 37 °C in air containing 5% CO_2. Non-phagocytosed parasites were removed by washing, and the infected cultures were incubated with the testing compounds (concentrations from 0·1 to 100 μM) and then cultured for 72 h in MEM plus glutamine (2 mM) and 20% inactive FCS. Compound activity was determined from the percentage reductions in amastigote number in treated *vs* untreated cultures in methanol-fixed and Giemsa-stained preparations. Values are the means of three separate determinations (González *et al*. 2005).

Ultrastructural alterations. The parasites were cultured at a density of 5×10^5 cells mL^{-1} in the corresponding medium, each of which contained the compounds being tested at the IC_{25} concentration. After 72 h, the cultures were centrifuged at 400 ***g*** for 10 min, and the pellets produced were washed in PBS and then incubated with 2% (v/v) formaldehyde/glutaraldehyde in 0·05 M cacodylate buffer (pH 7·4) for 24 h at 4 °C. The pellets were then prepared for TEM (Zeiss model, Barcelona, Spain) using a technique previously described (González *et al*. 2005).

Metabolite excretion. Cultures of *L. infantum* and *L. braziliensis* promastigotes (initial concentration 5×10^5 cells mL^{-1}) received the IC_{25} of the compounds (except for control cultures). After incubation for 72 h at 28 °C the cells were centrifuged at 400 ***g*** for 10 min. The supernatants were collected to determine the excreted metabolites by ^{1}H-NMR, and chemical shifts were expressed in ppm, using sodium 2,2-dimethyl-2-silapentane-5-sulphonate as the reference signal. The chemical displacements used to identify the respective metabolites were consistent with those described previously by some of the authors (Fernández-Becerra *et al*. 1997).

Fe-SOD enzymatic inhibition. Parasite cells were collected at the logarithmic growth phase by centrifugation (400 ***g*** for 10 min at room temperature) and then the pellet of cells (0·5–0·6 g wet weight mL^{-1}) was suspended in 25 mL of MTL not enriched with fetal bovine serum (FBS) and cultured at 26 °C for 24 h.

After that, the culture of promastigotes was centrifuged (400 ***g*** for 10 min) and the supernatant filtered (Minisart®, 0·2 μm). The filtered supernatant was subjected to ice-cold ammonium sulphate precipitation between 35–85% salt concentration

https://doi.org/10.1017/S0031182014000201 Published online by Cambridge University Press

and the resulting precipitate was dissolved in 2·5 mL of distilled water and de-salted by chromatography in Sephadex G-25 column (GE Healthcare Life Sciences®, PD 10 column), previously equilibrated with 25 mL of distilled water, bringing it to a final volume of 3·5 mL (Longoni *et al*. 2013). The protein content were quantified using the Sigma Bradford test, which uses BSA as a standard (no trace ability was certified for the BSA standard, Bradford, 1976).

Iron and copper–zinc superoxide dismutases (Fe-SOD and CuZn-SOD) activities were determined using a method previously described (Beyer and Fridovich, 1987) which measures the reduction in nitroblue tetrazolium (NBT) by superoxide ions. Into each bucket, 845 μL of stock solution [3 mL of L-metionine (300 mg, 10 mL^{-1}), 2 mL of NBT (1·41 mg, 10 mL^{-1}) and 1·5 mL of Triton X-100 1% (v/v)] were added, along with 30 μL of the parasite homogenate fraction, 10 μL of riboflavine (0·44 mg, 10 mL^{-1}), and an equivalent volume of the different concentrations of the compounds tested. Five different concentrations were used for each product, from 1 to 100 μM. In the control experiment the volume was made up to 1000 μL with 50 mM potassium phosphate buffer (pH 7·8, 3 mL), and 30 μL of the parasite homogenate fraction were added to the mixtures containing the compounds. Then, the absorbance (A_0) was measured at 560 nm in a spectrophotometer. Following this, each bucket was illuminated with UV light for 10 min under constant stirring and the absorbance (A_1) was again measured. Human CuZn-SOD and substrates used in these assays were obtained from Sigma Chemical Co. Resulting data were analysed using the Newman–Keuls test.

Molecular modelling. Molecular modelling studies were carried out using the AMBER (Case *et al*. 2005) method implemented in the HyperChem 8.0 package (Hypercube Inc., FL, USA), modified by the inclusion of appropriate parameters (Miranda *et al*. 2004). Starting structures for compounds **1–4** were built using HyperChem's capabilities. Their geometry was minimized to a maximum energy gradient of 0·1 kcal/(Å mol) with the AMBER force field, using the Polak-Ribière (conjugate gradient) minimizer, and a 'simulated annealing' procedure was used to cover all conformational space. The most stable extended geometry was always used in all calculations of interaction with the enzyme. To mimic the conditions used in the activity measurements, i.e. water as solvent, all calculations were carried out *in vacuo* with a distance-dependent dielectric constant value. In the absence of explicit solvent molecules, a distance-dependent dielectric factor qualitatively simulates the presence of water, as it takes into account the fact that the intermolecular electrostatic interactions should die off more rapidly with distance than in the gas phase (Reviriego *et al*. 2008). The same results can be obtained using a constant dielectric factor greater than 1. We chose to use a distance-dependent dielectric constant ($\varepsilon = 4$ R_{ij}) as this was the method used to develop the AMBER force field (Cornell *et al*. 1995). Charge assignations for all atoms were done by means of *ab initio* calculations using the STO-3G basis set, as it is compatible with the AMBER force field, prior to energy minimization using AMBER. The Fe-SOD enzyme structure was obtained from the Brookhaven protein data bank (2gpc entry) and its energy minimized in the same way. Interaction studies were done starting from structures having the compound positioned in the border of the enzyme cavity. To study different possible interactions of the enzyme's iron atom with any of the nitrogen atoms, entry into the cavity was forced using a restraint on the selected N-Fe distance, starting from 0·15 nm and slowly decreasing this distance, and allowing the complex to achieve the minimum energy conformation with no restraints for all the small driving steps, using the same conditions mentioned above.

RESULTS AND DISCUSSION

We report now on the results obtained concerning the toxic activity of the selected macrocyclic polyamines against two species of Leishmania (*L. infantum* and *L. braziliensis*).

In vitro *antileishmanial evaluation*

We measured the *in vitro* biological activity of compounds **1–4** on both extra- and intracellular forms of the parasites. Extracellular forms are more commonly used due to ease of working with them, but are less indicative of leishmanicidal activity. Use of intracellular forms is more cumbersome but gives more accurate results, as they are converted to amastigotes in vertebrate host cells (Sánchez-Moreno *et al*. 2012*a*). Intracellular assays were performed by infecting macrophage cells with promastigotes, which transformed into amastigotes within 1 day after infection. Tables 1 and 2 show the IC_{50} values obtained after 72 h of exposure for both *L. infantum* and *L. braziliensis*. Toxicity values against J774.2 macrophage after 72 h of culture were also calculated, and the selectivity indices (SI = IC_{50} macrophages toxicity/IC_{50} activity of extracellular or intracellular forms of the parasite) are shown in the last two columns of Tables 1 and 2. Results obtained for the reference drug glucantime were included for comparison.

It was shown that the leishmanicidal activities against both the extra- and intracellular forms of the parasites by the bicyclic polyamine **1** and the N-pyrazole methylsubstituted monocyclic polyamine **2** were, in all cases, higher than those seen

https://doi.org/10.1017/S0031182014000201 Published online by Cambridge University Press

Table 1. *In vitro* activity, toxicity and selectivity index for the macrocyclic polyamines **1–4** on extra- and intracellular forms of *L. infantum*

	Activity IC_{50} (μM)[a]			Selectivity index[c]	
Compounds	Promastigote forms	Intracellular amastigote forms	[b]Macrophage toxicity IC_{50}	Promastigote forms	Intracellular amastigote forms
Glucantime	18·0 ± 3·1	24·2 ± 2·6	15·2 ± 1·0	0·8	0·6
1	6·9 ± 0·2	12·2 ± 1·3	179·1 ± 12·8	25·9 (32)	14·7 (25)
2	12·0 ± 1·0	18·5 ± 0·9	218·5 ± 16·2	18·2 (23)	11·8 (20)
3	33·3 ± 2·3	16·2 ± 0·7	95·4 ± 7·6	2·9 (4)	5·9 (10)
4	20·5 ± 1·5	22·1 ± 1·5	41·8 ± 0·5	2·0 (2·5)	1·9 (3)

Results are averages of three separate determinations.
[a] IC_{50} is the concentration required to give 50% inhibition, calculated by linear regression analysis from the K_c values at the concentrations employed (1, 10, 25, 50 and 100 μM).
[b] Against J774.2 macrophages after 72 h of culture.
[c] Selectivity index = IC_{50} macrophages toxicity/IC_{50} activity on extracellular or intracellular forms of the parasite. In parentheses: number of times the compound SI exceeded the reference drug SI.

Table 2. *In vitro* activity, toxicity and selectivity index for the macrocyclic polyamines **1–4** on extra- and intracellular forms of *L. braziliensis*

	Activity IC_{50} (μM)[a]			Selectivity index[c]	
Compounds	Promastigote forms	Intracellular amastigote forms	[b]Macrophage toxicity IC_{50}	Promastigote forms	Intracellular amastigote forms
Glucantime	25·6 ± 1·6	30·4 ± 6·1	15·2 ± 1·0	0·6	0·5
1	13·4 ± 0·1	11·7 ± 0·7	179·1 ± 12·8	13·4 (22)	15·3 (31)
2	9·9 ± 0·5	5·8 ± 0·6	218·5 ± 16·2	22·1 (37)	37·7 (75)
3	16·2 ± 0·9	9·6 ± 1·0	95·4 ± 7·6	5·9 (10)	9·9 (20)
4	29·6 ± 3·0	8·1 ± 0·4	41·8 ± 0·5	1·4 (2)	5·2 (10)

Results are averages of three separate determinations.
[a] IC_{50} = the concentration required to give 50% inhibition, calculated by linear regression analysis from the K_c values at the concentrations employed (1, 10, 25, 50 and 100 μM).
[b] Against J774·2 macrophages after 72 h of culture.
[c] Selectivity index = IC_{50} macrophages toxicity/IC_{50} activity on extracellular or intracellular forms of the parasite. In parentheses: number of times the compound SI exceeded the reference drug SI.

with glucantime, while more random values were found for the N-benzylsubstituted analogue **3** and the monocyclic polyamine octylsubstituted on the side-chain nitrogen **4**. However, more interesting are the toxicity data in mammalian cells, since all four compounds tested were found to be much less toxic for macrophages than the reference drug. Thus, compounds **1** and **2** were 12-fold and 14-fold respectively less toxic than glucantime, and even the most toxic among them, **4**, was 3-fold more benign. Toxicity values substantially influence the more informative selectivity index (SI) data, so the best values were again obtained for compounds **1** and **2**. In tests performed on *L. infantum* species, SI exceeded that of the reference drug by 32- and 25-fold for the extra- and intracellular forms in the case of **1**, and by 23- and 20-fold with **2**, while on *L. braziliensis*, the respective values obtained were 22- and 31-fold with **1** and 37- and 75-fold with **2**. It should be noted that a SI value exceeding 20-fold that of the reference drug is one of the usual basic criteria for considering primarily screened compounds as candidates for more advanced testing *in vitro* and in animal models (Nwaka *et al*. 2011). On the contrary, the N-octylsubstituted compound **4** was the least efficient (2·5- and 3-fold on *L. infantum* and 2- and 10-fold on *L. braziliensis*), whereas **3** gave intermediate values between the **1**/**2** pair and **4**. *Leishmania braziliensis* showed a higher susceptibility for **2**, since its SI was 75-fold that of glucantime in the more indicative intracellular amastigote test, a much better result than that found for *L. infantum*.

The tests described above represent only a first crude approach to the leishmanicidal properties of the compounds assayed. In order to gain better insight into the activity of compounds **1–3**, their effect on the infectivity and intracellular replication of amastigotes was subsequently determined. In accordance with the usual working procedure, polyamine **4** was not included in this second stage, due to

https://doi.org/10.1017/S0031182014000201 Published online by Cambridge University Press

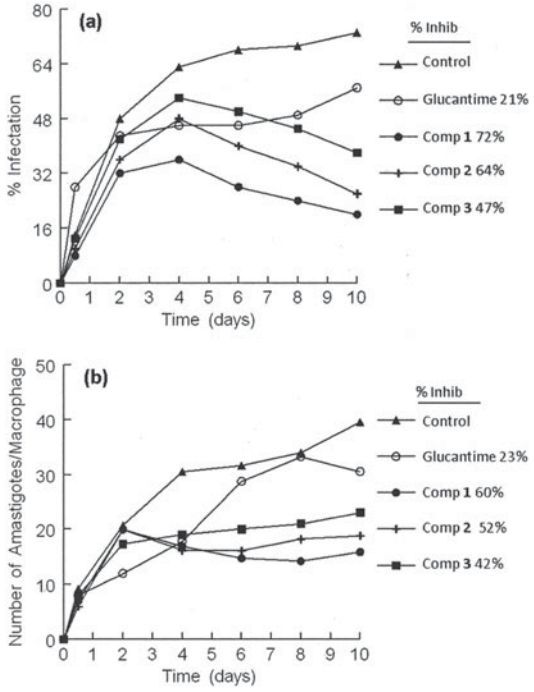

Fig. 2. Effect of pyrazole-containing polyamine macrocycles **1–3** on the infection and growth rates of *Leishmania* spp.: (a): rate of infection of *L. infantum*, (b): mean number of amastigotes of *L. infantum* per infected J774 A.2 macrophage cells (at IC_{25} conc). Values are means of three separate experiments.

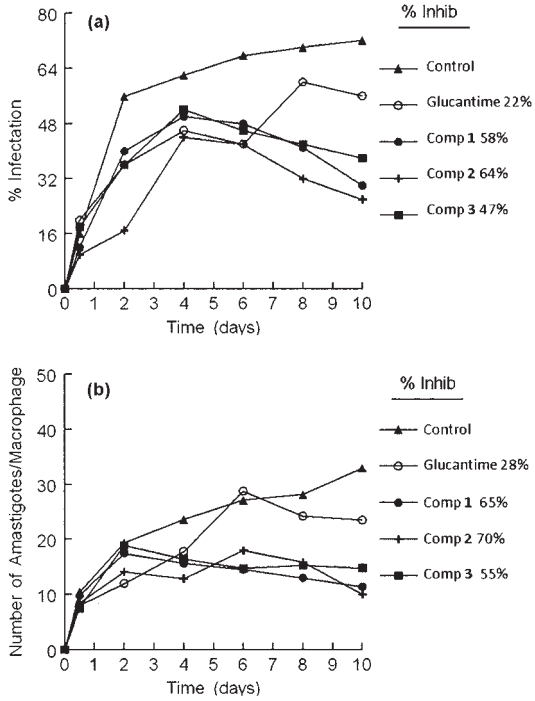

Fig. 3. Effect of pyrazole-containing polyamine macrocycles **1–3** on the infection and growth rates of *Leishmania* spp.: (a): rate of infection of *L. braziliensis*, (b): mean number of amastigotes of *L. braziliensis* per infected J774 A.2 macrophage cells (at IC_{25} conc). Values are means of three separate experiments.

the poor SI results obtained. Macrophage cells were grown and infected with promastigotes in the stationary phase. The parasites invaded the cells and underwent morphological conversion to amastigotes within 1 day after infection. On day 10, the rate of host cell infection reached its maximum (control experiment). We used the IC_{25} of each product as the test dosage.

As shown in Fig. 2a, when macrocycles **1–3** were added to macrophages infected with *L. infantum* promastigotes, the infection rate decreased significantly with respect to the control and, furthermore, the three compounds were also more effective in decreasing infectivity than glucantime (72, 64 and 47% for **1, 2** and **3** respectively, *vs* only 21% for the reference drug). The bicyclic polyamine **1** and the monocyclic N-methylsubstituted pyrazole polyamine **2** were clearly more efficient than the N-benzylsubstituted compound **3**. A measure of the average number of amastigotes per infected macrophage (Fig. 2b) led to similar conclusions: all three compounds were more effective than glucantime (with only a 23% decrease), and their order of effectiveness followed the same pattern as that seen in the infectivity measures, although the differences between them were less pronounced (60, 52 and 42%) for **1, 2** and **3**, respectively).

The same experiment was performed with *L. braziliensis*, and the results obtained concerning infection rates (a) and amastigote numbers (b) can be observed in Fig. 3. In both cases, the three compounds were also more effective than glucantime, and also in both cases the order of effectiveness was now **2** > **1** > **3**, since the infectivity rates calculated from Fig. 3 were: 64, 58, 47 and 22%; and the decrease in amastigote numbers was: 70, 65, 55 and 28% for **2, 1, 3** and glucantime respectively.

If we now compare the results obtained for both *Leishmania* species, it can be concluded that, in accordance with the SI values displayed in Tables 1 and 2, the N-methylsubstituted polyamine **2** is more efficient in *L. braziliensis* with respect to *L. infantum*, and the N-benzylsubstituted polyamine **3** is the least active in both species.

The leishmanicidal activity shown by compounds **1–3** should lead to relevant damage to parasite cells. Therefore, we performed a transmission electron microscopy (TEM) study on the promastigote forms of *L. infantum* and *L. braziliensis* treated with **1–3**. As expected, significant morphological alterations were observed compared with untreated control cells. Figure 4 displays structural features observed in control and treated cells of both Leishmania species. Treatment with **1** and **2** led to remarkable morphological alterations involving deep vacuolization and loss of cytoplasmic content (Fig. 4, plates b and c in both charts). In most cases, much of the cytoplasm was filled with huge empty or granulated vacuoles, some of them electron-dense, that were occupying nearly all the cytoplasmic space of the promastigotes,

https://doi.org/10.1017/S0031182014000201 Published online by Cambridge University Press

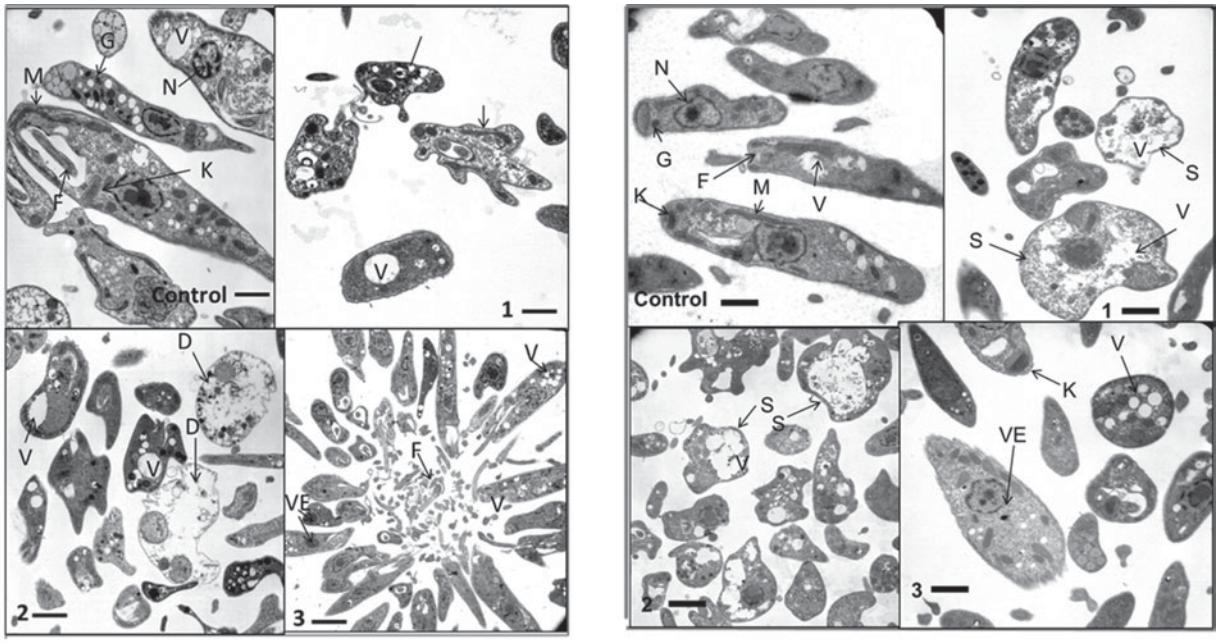

Fig. 4. Chart 1: Ultrastructural alterations observed by TEM in promastigotes of *L. infantum* treated with compounds **1–3**. (a) Control parasite (scale bar: 1·00 μm). (b) **Comp 1** (scale bar: 1·00 μm), (c) **Comp 2**, (scale bar: 1·59 μm), (d) **Comp 3** (scale bar: 2·33 μm). Promastigotes after treatment with the respective compounds. Abbreviations: dead parasites (D), flagellum (F), glycosomes (G), kinetoplast (K), mitochondrion (M), nucleus (N), vacuoles (V), electron dense vesicles (VE), star-shaped promastigotes (single arrow). Chart 2: Ultrastructural alterations observed by TEM in promastigotes of *L. braziliensis* treated with compounds **1–3**. (a) Control parasite (scale bar: 1·00 μm). (b) **Comp 1** (scale bar: 1·00 μm), (c) **Comp 2**, (scale bar: 1·59 μm), (d) **Comp 3** (scale bar: 1·00 μm). Promastigotes after treatment with the respective compounds. Abbreviations: flagellum (F), glycosomes (G), kinetoplast (K), mitochondrion (M), nucleus (N), swollen promastigotes (S), vacuoles (V), electron dense vesicles (VE).

and generated very swollen cytoplasmic forms. In fact, the usual cytoplasmic organelles could hardly be found. Some parasites were dead, or appeared as very swollen or were ready to burst. Parasites treated with compound **3** presented scarcer alterations (Fig. 4, plate d), and many of them coalesced to rosettes, although some were also vacuolated, presented small electron-dense vesicles or showed modified kinetoplasts. On the basis of these data, macrocyclic polyamines **1** and **2** were confirmed to be especially harmful to both *L. infantum* and *L. braziliensis* species.

Metabolite excretion

Since trypanosomatids are unable to completely degrade glucose to CO_2, they excrete a considerable portion of its hexose skeleton as partially oxidized fragments in the form of fermented metabolites, whose nature and percentage depend on the pathway used for glucose metabolism (Ginger, 2005; Bringaud *et al*. 2006). The catabolism products in Leishmania are usually CO_2, succinate, acetate, pyruvate, **D**-lactate, **L**-alanine, and, to a lesser extent, ethanol (Cazzulo, 1992). Detection of large amounts of succinate as a major end product is a usual feature, because it rules on glycosomal redox balance, enabling reoxidation of NADH produced in the glycolytic pathway. Succinic fermentation requires only half of the phosphoenolpyruvate produced to maintain the NAD^+/NADH balance, and the remaining pyruvate is converted inside the mitochondrion and the cytosol into acetate, **L**-lactate, **L**-alanine or ethanol according to the degradation pathway followed by each species (Michels *et al*. 2006).

In order to obtain some information concerning the effect of the tested compounds on glucose metabolism in the parasites, we registered the ^{1}H-NMR spectra of promastigotes from *L. infantum* and *L. braziliensis* after treatment with compounds **1–3**, and the final excretion products were identified qualitatively and quantitatively. The results were compared with those found with promastigotes maintained in a cell-free medium (control) for 3 days after inoculation with the parasite. The characteristic presence of acetate, **D**-lactate, succinate, **L**-alanine and ethanol was confirmed in the control experiments performed on both species. As expected, succinate and acetate were the most abundant end products identified. However, after treatment of the parasites with **1–3**, the excretion of catabolites was substantially altered at the dosages

https://doi.org/10.1017/S0031182014000201 Published online by Cambridge University Press

Table 3. Variation in the height of peaks corresponding to catabolites excreted by *L. infantum* and *L. braziliensis* promastigote forms in the presence of macrocyclic polyamines **1–3** with respect to the control test[a]

Comp.	Eth	Lac	Ala	A	S	Pyr	Gly
	L. infantum[a]						
1	ND	−37%	−46%	−80%	−100%	+100%	+100%
2	ND	−20%	=	−40%	−29%	+80%	+100%
3	ND	=	=	+20%	+39%	ND	ND
	L. braziliensis[a]						
1	−100%	−33%	−100%	−100%	−100%	+73%	+100%
2	−100%	−27%	−26%	−80%	−100%	+100%	+66%
3	+37%	=	=	=	=	ND	ND

[a] Eth, ethanol; Lac, **D**-lactate; Ala, **L**-alanine; A, acetate; S, succinate; Pyr, pyruvate; Gly, glycine; (–), decreasing peak; (+), increasing peak; (=), no difference detected; (ND), peak undetected.

employed. Table 3 displays these modifications with respect to the control observed at the height of the spectral peaks corresponding to the most representative final excretion products. Marked differences in the catabolic pathway appeared, and that seemed to be connected with the leishmanicidal activity commented on above. The main features found for both species were substantial increases in the formation of pyruvate and glycine with the most active macrocyclic polyamines **1** and **2**, accompanied by corresponding decreases in succinate and acetate and, to a lesser extent, **D**-lactate. In *L. infantum*, the most active compound **1** increased pyruvate and glycine by 100%, and triggered widespread decreases in succinate, acetate, **D**-lactate and **L**-alanine by 100, 80, 37 and 46% respectively. Similar results were obtained with compound **2**, although with slightly smaller variations. In contrast, the less active compound **3** did not increase pyruvate nor glycine at all (they were not detected), but slightly increased succinate and acetate by 39 and 20% respectively, in sharp contrast with **1** and **2**. If we turn now to the results obtained with the *L. braziliensis* species, compounds **1** and **2** also substantially increased the formation of pyruvate (73 and 100% respectively) and glycine (100 and 66%), and decreased the production of succinate (100% in both cases), acetate, **D**-lactate and **L**-alanine, whereas with the less active compound **3** pyruvate and glycine were not detected and succinate, acetate, **L**-lactate and **L**-alanine did not experience any modifications with respect to the control. All these data could be interpreted on the basis of a change in the succinate and acetate pathways occurring in the presence of the most active compounds **1** and **2**. It is well known that acetate, **D**-lactate, **L**-alanine and ethanol originate from the transformation of PEP in pyruvate in the presence of pyruvate kinase or pyruvate phosphate dikinase (Bringaud *et al*. 2006). Therefore, it seems possible that compounds **1** and **2** were interacting with the pyruvate kinase enzymes and modifying the glucose metabolism of the parasite at the pyruvate stage. On the other hand, it is interesting to note that the decrease in succinate with compounds **1** and **2** is accompanied by the appearance of glycine, which is not present in the normal catabolism of the parasite. Those catabolic changes could also be related to a malfunction of the mitochondria, due to the redox stress produced by inhibition of the mitochondrion-resident Fe-SOD enzyme (Kirkinezos and Moraes, 2001), which should result in decrease of pyruvate metabolism and a consequent decrease of the succinate and acetate produced in mitochondria. These data appear to confirm that the severe modifications generated in organelles such as glycosomes or mitochondria by **1** and **2** are the ultimate reasons for the alterations observed in the excretion products of both species.

SOD enzymatic inhibition in the parasites and in human erythrocytes

Since we had found that the anti-*T. cruzi* activity of compounds **1–4** was accompanied by a remarkable inhibitory activity on the essential antioxidant enzyme Fe-SOD (Sánchez-Moreno *et al*. 2012*a*,*b*), we tested the effect of **1–4** on Fe-SOD isolated from *L. infantum* and *L. braziliensis* over a range of concentrations from 1 to 100 μM. We used promastigote forms of both species, which excreted Fe-SOD when cultured in a medium lacking inactive FBS (Longoni *et al*. 2013). The inhibition data obtained are displayed in Fig. 5, parts a and b, and the corresponding IC_{50} values are included in order to make interpretation of the results easier. For comparison, part c of Fig. 5 shows the effect of the same compounds on CuZn-SOD obtained from human erythrocytes. The most remarkable result was the significant inhibition of Fe-SOD activity found for **1–3**, whereas their inhibition of human CuZn-SOD was clearly lower. If we consider the IC_{50} calculated for *L. infantum*, inhibition of Fe-SOD by compounds **1–3** was respectively 4·6-, 6·2- and 2·8-fold

https://doi.org/10.1017/S0031182014000201 Published online by Cambridge University Press

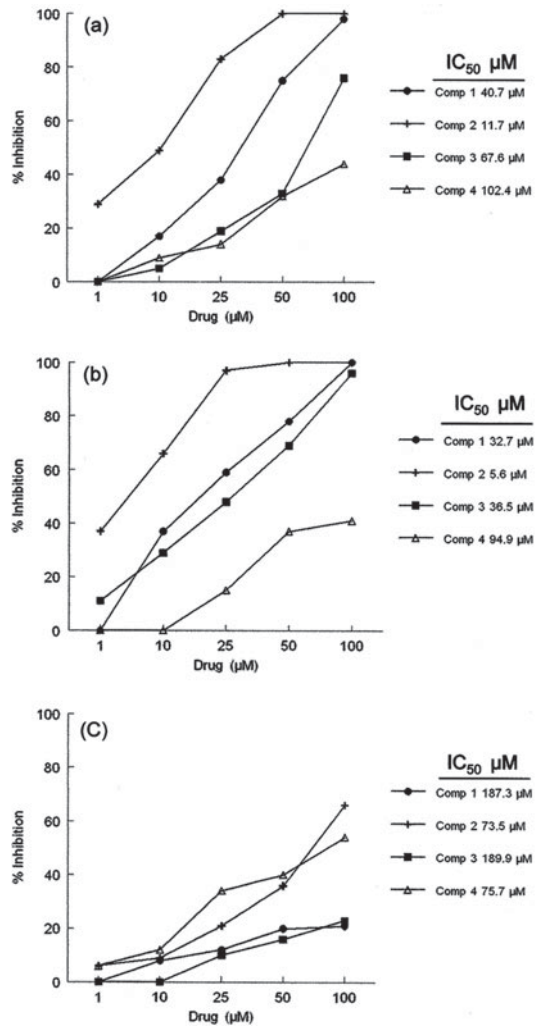

Fig. 5. *In vitro* inhibition (%) of Fe-SOD of: (a) *Leishmania infantum* and (b) *Leishmania braziliensis* promastigotes by compounds **1–4**. (c) *In vitro* inhibition of CuZn-SOD in human erythrocytes by compounds **1–4**. Values are the average of three separate determinations. Differences between the activities of the control homogenate and those incubated with compounds **1–4** were obtained according to the Newman–Keuls test. [a]IC_{50} = the concentration required to give 50% inhibition was calculated by linear regression analysis from the K_c values at the concentrations employed (1, 10, 25, 50 and 100 μM).

higher than inhibition of CuZn-SOD, and respective values of 5·7-, 13·1- and 5·2-fold higher were obtained in the case of *L. braziliensis*. On the contrary, the N-octyl derivative **4** was not selective at all, and resulted in even less inhibition of Fe-SOD than of the CuZn enzyme, in concordance with the poor *in vitro* activity results noted before. It can also be concluded that compound **2** is a more efficient Fe-SOD inhibitor in *L. braziliensis* than in *L. infantum* (IC_{50} 5·6 and 11·7 μM, respectively). It is also interesting to note that the Fe-SOD inhibition rankings are **2**>**1**>**3**>>>**4**, suggesting a relationship between the inhibitory ability and the hindrance caused by the substituents in the neighbourhood of

Table 4. *Ab initio* calculated charges on the nitrogen atoms of compounds **1–4**

Comp.	$N_{pyrazole}$	N_β	N_ε
1	−0·159	−0·327	−0·279
2	−0·183	−0·324	−0·332
3	−0·186	−0·325	−0·331
4	−0·175	−0·325	−0·278

Table 5. Calculated distances between the iron atom in the active site of the Fe-SOD enzyme and the different nitrogen atoms of compounds **1–4**

	Distance (nm)		
Comp.	Fe-$N_{pyrazole}$	Fe-N_β	Fe-N_ε
1	0·777	0·361	0·483
2	0·669	0·553	0·391
3	0·882	0·564	0·392
4	0·804	0·545	0·702

the macrocycle side-chain nitrogens, since the methyl groups in **2** are less bulky than the benzyl groups of **3**, and much less bulky than the octyl groups attached to **4**. Compound **1**, as an unsubstituted bicyclic macrocycle, should presumably approach the active site core of the enzyme with more difficulty than the monocyclic compound **2**. That could be in accordance with some kind of interaction of the macrocycle nitrogens with the active sites of the enzyme in both *Leishmania* species. As has been pointed out, the modification of Fe-SOD activity by a particular compound should take place by modifying the coordination geometry of the iron atoms, reorganizing the active sites H-bonding network (Yikilmaz *et al*. 2006) or reducing the cooperative interaction between the two monomers of the enzyme (Muñoz *et al*. 2005).

In order to obtain more information, molecular modelling calculations on the mode of interaction of the tested compounds with the enzyme were performed. Fe-SOD enzymes are dimeric forms in which either of the two monomers contains an iron atom. While the CuZn-SOD enzyme of mammals has the metal active sites located deeper inside the monomers, the active sites of the parasite Fe-SOD are closer to the interface between the two subunits, so that the channel opening in the inner part of the dimer is the obvious place to locate a molecule in search of interaction with the iron environment (Abreu and Cabelli, 2010). Therefore, the macrocycles were positioned inside the cavity. However, there are three different types of nitrogen atoms able to interact: that of the pyrazole ring and those located in the β and ε positions of the connecting side chains. Table 4 displays the Milliken net charges obtained

https://doi.org/10.1017/S0031182014000201 Published online by Cambridge University Press

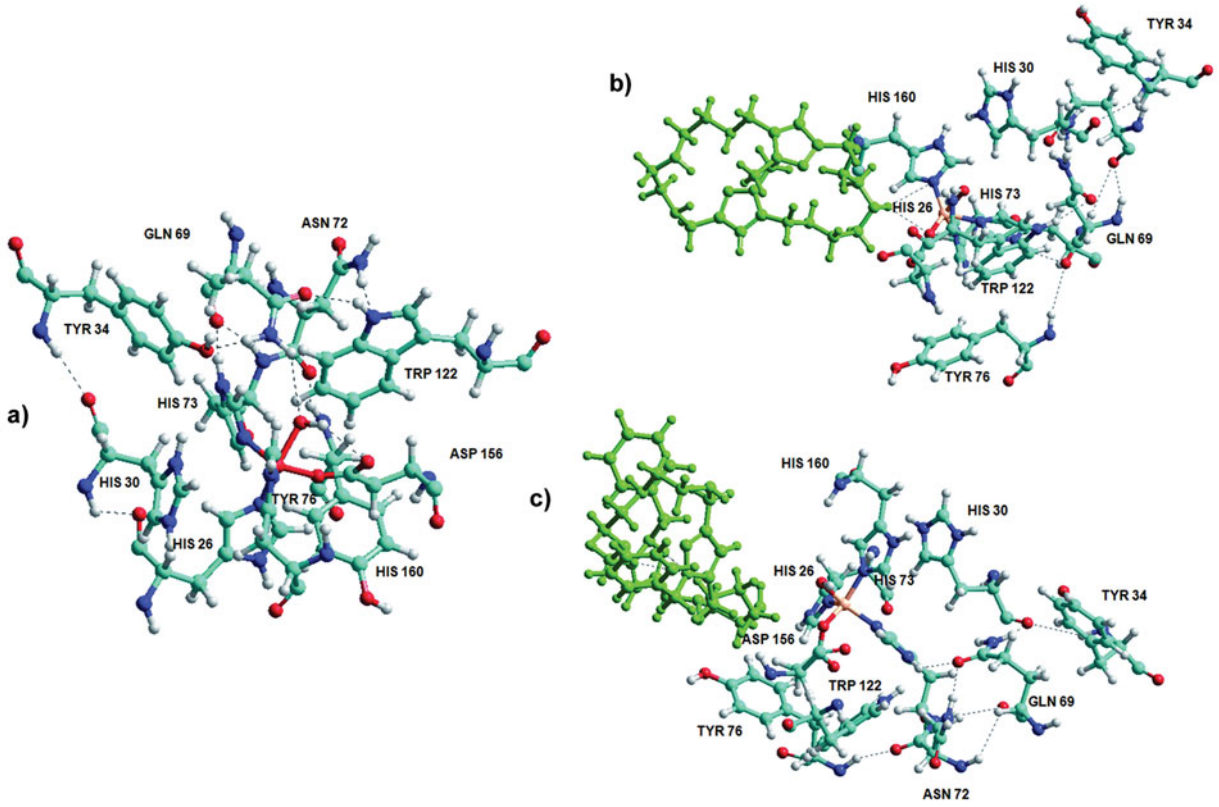

Fig. 6. (a) Molecular model of the free Fe-SOD enzyme active site with its supporting network of hydrogen bonds displayed as dashed lines. (b) and (c) Molecular models of the Fe-SOD enzyme active site with the $N_{pyrazole}$ methyl substituted macrocycle **2** (b) and the $N_{pyrazole}$ benzyl substituted macrocycle **3** (c) embedded in the proximity of the iron atom, and the modified hydrogen-bonding networks.

for the different nitrogens by means of *ab initio* calculations using the STO-3G basis set (Leite, 1998). It was shown that in all four compounds the pyrazole nitrogens exhibited the lowest basicity whereas the $\beta-$nitrogens were the most basic in **1** and **4**, but not in **2** and **3**. Consequently, the approach mode of each molecule to the active centre should take place through the polyamine side chains, instead of the pyrazole units. On that basis, and using the AMBER force field implemented in HyperChem, we applied a methodology previously developed by us (Sánchez-Moreno *et al*. 2012*b*) to the structure of a Fe-SOD enzyme model obtained from the Brookhaven Protein Data Bank 2gpc entry. First, the most favoured distance between the iron atom of one subunit and the three different nitrogens under consideration was calculated for compounds **1–4** (Table 5). In all four cases the pyrazole nitrogens were located further from the metal than those at the side-chains, in accordance with the charge data detailed above. On the other hand, all the nitrogen atoms of the bulky N-octyl substituted macrocycle **4** stood too far from the metal environment to effectively modify its geometry, and this fact should be connected with the very poor inhibitory activity of compound **4** against Fe-SOD measured experimentally. The unsubstituted bicyclic polyamine **1** showed the closest approach to the iron atom (0·361 nm), which took place through the N_{β} nitrogen, and the $N_{pyrazole}$ substituted compounds **2** and **3** afforded their best results through their N_{ε} nitrogens. These distances are too large to enable a direct Fe·····N interaction, but they are suitable to modify the arrangement of the aminoacids involved in the active site core. From these data, it seems that the side-chain nitrogens are better able to affect the iron atom environment, and that the presence of substituents on the macrocycle influences its interaction with that environment.

A further step should involve consideration of the effect caused by the tested compounds on the hydrogen bonding network wrapping the metal atom. In Fe-SOD, the metal appears as a five-coordinated active site ligated by three histidine units, an aspartate group and an axial H_2O or HO^- ligand supported by an essential hydrogen bonding network comprising diverse amino acids (Miller *et al*. 2005). Specifically, the coordinated molecule engages in a H-bond with Asp156, and another H-bond engages with Gln69 (Yikilmaz *et al*. 2006). The H_2O/HO^- ligand and its hydrogen-bonding partners are essential for tuning the antioxidant activity of Fe-SOD (Stallings *et al*. 1991; Yikilmaz *et al*. 2002), since it acts as a proton donor/acceptor and facilitates

https://doi.org/10.1017/S0031182014000201 Published online by Cambridge University Press

the release of peroxide generated by the reduction of the substrate (Han *et al*. 2002). On that basis, we modelled the active site moiety of the Fe-SOD enzyme as shown in Fig. 6a, in which the hydrogen bonding system is displayed as dashed lines, the H_2O ligand appears in the foreground and the key interactions with Gln69 and Asp160 are clearly seen.

The best Fe-SOD inhibitor in both *L. infantum* and *L. braziliensis*, **2**, was selected for estimating its effect on the active site environment. The approach of **2** to the active site confirmed that the most basic β-nitrogen pointed towards the metal ion in the most favoured disposition (Fig. 6b). As a consequence, the amino acids surrounding the iron atom were displaced apart from their initial positions, the hydrogen bonding pattern appeared completely distorted, and Gln69 was located too far from the HO^- group to form a stable hydrogen bond. Instead, the β-nitrogen of the macrocycle was linked through two hydrogen bonds to the imidazole nitrogen of the His160 unit and to one oxygen atom of the Asp156 molecule, two amino acids involved in the coordination sphere of the iron atom. We think that these results could explain in part the enzyme deactivation found experimentally. As a term of comparison, the same treatment was given to the poorly inhibitory compound **3**, in which the only difference is replacement of the pyrazole methyl group for the more bulky benzyl substituent. The most favoured disposition is shown in Fig. 6c. It can be seen that, although the H-bonding net is also distorted and Gln69 is moved away from its usual location, the drug molecule is placed further away from the metal environment than in the case of **2** and the two hydrogen bonds that link compound **2** with the coordination sphere are missing. Therefore, steric hindrance originating from the macrocycle's substituents should affect its ability to inhibit the Fe-SOD enzyme. Those catabolic changes could be also related to a malfunction of the mitochondria, due to the redox stress produced by inhibition of the mitochondrion-resident Fe-SOD enzyme (Kirkinezos and Moraes, 2001), which should result in decrease of pyruvate metabolism and a consequent decrease of the succinate and acetate produced in mitochondria.

From all the results detailed above, we conclude that the macrocyclic polyamines **1** and **2** show interesting *in vitro* leishmanicidal activity which seems to be related to their inhibitory ability against the Fe-SOD of the parasite. Furthermore, as discussed above, redox stress derived from Fe-SOD inhibition could also explain the catabolic changes observed. On that basis, we think that they fulfil the requirements needed to justify a more detailed investigation into the nature of the mechanisms involved in its activity patterns, and furthermore, that they could be considered as candidates for study of antiparasitic activity at a higher level.

ACKNOWLEDGEMENTS

The authors thank the Departamento de Analisis of the Centro Nacional de Química Orgánica Manuel Lora-Tamayo (C.S.I.C.) for the analysis performed concerning the purity of the compounds tested. We are also grateful to the transmission electron microscopy and nuclear magnetic resonance spectroscopy services of the CIC-University of Granada for their contribution to the studies on ultrastructural alterations and catabolism.

FINANCIAL SUPPORT

Financial support from the Spanish Ministerio de Ciencia e Innovacion (CTQ2009-14288-C04-01 and Consolider Ingenio CSD2010-00065), and from the Santander-Universidad Complutense Research Programme (GR35/10-A-921371) is also acknowledged.

REFERENCES

Abreu, I. A. and Cabelli, D. E. (2010). Superoxide dismutases: a review of the metal-associated mechanistic variations. *Biochimica et Biophysica Acta* **1804**, 263–274.

Amato, V. S., Tuon, F. F., Siqueira, A. M., Nicodemo, A. C. and Neto, V. A. (2007). Treatment of mucosal leishmaniasis in Latin America: systematic review. *American Journal of Tropical Medicine and Hygiene* **77**, 266–274.

Arán, V. J., Kumar, M., Molina, J., Lamarque, L., Navarro, P., García-España, E., Ramírez, J. A., Luis, S. V. and Escuder, B. (1999). Synthesis and protonation behavior of 26-membered oxaaza- and polyazamacrocycles containing two heteroaromatic units of 3,5-disubstituted pyrazole or 1-benzylpyrazole: a potentiometric and ^{1}H and ^{13}C NMR study. *Journal of Organic Chemistry* **64**, 6135–6146.

Beyer, W. F. and Fridovich, I. (1987). Assaying for superoxide dismutase activity: some large consequences of minor changes in conditions. *Analytical Biochemistry* **161**, 559–566.

Bradford, M. M. (1976). A rapid and sensitive method for the quantitation of microgram quantities of protein utilizing the principle of protein-dye binding. *Analytical Biochemistry* **72**, 248–254.

Bringaud, F., Riviere, L. and Coustou, V. (2006). Energy metabolism of Trypanosomatids: adaptation to available carbon sources. *Molecular and Biochemical Parasitology* **149**, 1–9.

Case, D. A., Cheatham, T. E., Darden, T., Gohlke, H., Luo, R., Merz, K. M., Jr., Onufriev, A., Simmerling, C., Wang, B. and Woods, R. J. (2005). The Amber biomolecular simulation programs. *Journal of Computational Chemistry* **26**, 1668–1688.

Cazzulo, J. J. (1992). Aerobic fermentation of glucose by trypanosomatids. *FASEB Journal* **6**, 3153–3161.

Chappuis, F., Sundar, S., Hailu, A., Ghalib, H., Rijal, S., Peeling, R. W., Alvar, J. and Boelaert, M. (2007). Visceral leishmaniasis: what are the needs for diagnosis, treatment and control? *Nature Reviews Microbiology* **5**, 873–882.

Cornell, W. D., Cieplak, P., Bayly, C. I., Gould, I. R., Merz, K. M., Ferguson, D. M., Spellmeyer, D. C., Fox, T., Caldwell, J. W. and Kollman, P. A. (1995). A second generation force field for the simulation of proteins, nucleic acids, and organic molecules. *Journal of the American Chemical Society* **117**, 5179–5197.

Croft, S. L., Sundar, S. and Fairlamb, A. H. (2006). Drug resistance in leishmaniasis. *Clinical Microbiology Reviews* **19**, 111–126.

Deschacht, M., Van Assche, T., Hendrickx, S., Bult, H., Maes, L. and Cos, P. (2012). Role of oxidative stress and apoptosis in the cellular response of murine macrophages upon *Leishmania* infection. *Parasitology* **139**, 1429–1437.

Fernández-Becerra, C., Sánchez-Moreno, M., Osuna, A. and Opperdoes, F. R. (1997). Comparative aspects of energy metabolism in plant trypanosomatids. *Journal of Eukaryotic Microbiology* **44**, 523–529.

Ginger, M. (2005). Trypanosomatid biology and euglenozoan evolution: new insights and shifting paradigms revealed through genome sequencing. *Protist* **156**, 377–392.

González, P., Marín, C., Rodríguez-González, I., Hitos, A. B., Rosales, M. J., Reina, M., Díaz, J. G., González-Coloma, A. and Sánchez-Moreno, M. (2005). *In vitro* activity of C_{20}-diterpenoid alkaloid derivatives in promastigotes and intracellular amastigotes of *Leishmania infantum*. *International Journal of Antimicrobial Agents* **25**, 136–141.

https://doi.org/10.1017/S0031182014000201 Published online by Cambridge University Press

Guerra, J. A., Prestes, S. R., Silveira, H., Coelho, L. I. A. R., Gama, P., Moura, A., Amato, V., Barbosa, M. G. V. and Ferreira, L. C. L. (2011). Mucosal leishmaniasis caused by *Leishmania* (*Viannia*) *braziliensis* and *Leishmania* (*Viannia*) *guyanensis* in the Brazilian Amazon. *PLoS Neglected Tropical Diseases* **5**, e980. doi: 10.1371/journal.pntd.0000980637-46.

Han, W. G., Lovell, T. and Noodleman, L. (2002). Coupled redox potentials in manganese and iron superoxide dismutases from reaction kinetics and density functional/electrostatics calculations. *Inorganic Chemistry* **41**, 205–218.

Hypercube, Inc. (n.d.) *HyperChem(TM) Professional 8.0*. Hypercube, Inc., Gainesville, FL, USA.

Kirkinezos, I. G. and Moraes, C. T. (2001). Reactive oxygen species and mitochondrial diseases. *Cell and Developmental Biology* **12**, 449–457.

Kumar, M., Bhalla, V. S. N., Kumar, V., Singh, M. and Singh, G. (2001). Synthesis of new macrocyclic polyaza compounds containing 1-methylpyrazole. *Journal of Inclusion Phenomena and Macrocyclic Chemistry* **39**, 241–245.

Lamarque, L., Navarro, P., Miranda, C., Arán, V. J., Ochoa, C., Escartí, F., García-España, E., Latorre, F., Luis, S. V. and Miravet, J. F. (2001). Dopamine interaction in the absence and in the presence of Cu^{2+} ions with macrocyclic and macrobicyclic polyamines containing pyrazole units. Crystal structure of $[Cu_2(L1)(H_2O)_2](ClO_4)_4$ and $[Cu_2(H_{-1}L3)](ClO_4)_3 \cdot 2H_2O$. *Journal of the American Chemical Society* **123**, 10560–10570.

Leite, S. R. A. (1998). Basicities of primary arylamines and calculated amine nitrogen electronic charges. *Eclética Química* **23**, 71–80.

Longoni, S. S., Sánchez-Moreno, M., Rivera-López, J. E. and Marín, C. (2013). *Leishmania infantum* excreted iron superoxide dismutase purification and its application to the diagnosis of canine Leishmaniasis. *Comparative Immunology, Microbiology and Infectious Diseases*. http://dx.doi.org/10.1016/j.cimid.2013.05.00415.

Lukes, J., Mauricio, I. L., Schönian, G. G., Dujardin, J. C., Soteriadou, K., Dedet, J. P., Kuhis, K., Tintaya, K. W. Q., Jirku, M., Chocholová, E., Haralambous, C., Pratlong, F., Obornik, M., Horák, A., Ayala, F. J. and Miles, M. A. (2007). Evolutionary and geographical history of the *Leishmania donovani* complex with a revision of current taxonomy. *Proceedings of the National Academy of Sciences USA* **104**, 9375–9380.

Marín, C., Ramírez-Macías, I., López-Céspedes, A., Olmo, F., Villegas, N., Díaz, J. G., Rosales, M. J., Gutiérrez-Sánchez, R. and Sánchez-Moreno, M. (2011). *In vitro* and *in vivo* trypanocidal activity of flavonoids from *Delphinium staphisagria* against Chagas disease. *Journal of Natural Products* **74**, 744–750.

Michels, P. A. M., Bringaud, F., Herman, M. and Hannaert, V. (2006). Metabolic functions of glycosomes in trypanosomatids. *Biochimica et Biophysica Acta* **1763**, 1463–1477.

Miller, A. F. (2004). Superoxide dismutases: active sites that save, but a protein that kills. *Current Opinion in Chemical Biology* **8**, 162–168.

Miller, A. F., Sorkin, D. L. and Padmakumar, K. (2005). Anion binding properties of reduced and oxidized iron-containing superoxide dismutase reveal no requirement for tyrosine 34. *Biochemistry* **44**, 5969–5981.

Miranda, C., Escartí, F., Lamarque, L., Yunta, M. J. R., Navarro, P., García-España, E. and Jimeno, M. L. (2004). New ^{1}H-pyrazole-containing polyamine receptors able to complex L-glutamate in water at physiological pH values. *Journal of the American Chemical Society* **126**, 823–833.

Muñoz, I. G., Morán, J. F., Becana, M. and Montoya, G. (2005). The crystal structure of an eukaryotic iron superoxide dismutase suggests intersubunit cooperation during catalysis. *Protein Science* **14**, 387–394.

Nwaka, S., Besson, D., Ramirez, B., Maes, L., Matheeussen, A., Bickle, Q., Mansour, N. R., Yousif, F., Townson, S., Gokool, S., Cho-Ngwa, F., Samje, M., Misra-Bhattacharya, S., Murthy, P. K., Fakorede, F., Paris, J. M., Yeates, C., Ridley, R., Van Voorhis, W. C. and Geary, T. (2011). Integrated dataset of screening hits against multiple neglected disease pathogens. *PLoS Neglected Tropical Diseases* **5**, e1412. doi: 10.1371/journal.pntd.0001412.

Palumbo, E. (2009). Current treatment for cutaneous leishmaniasis: a review. *American Journal of Therapeutics* **16**, 178–182.

Perrin, D. D., Armarego, W. L. F. and Perrin, D. R. (1980). *Purification of Laboratory Chemicals*. Pergamon Press, Oxford, UK.

Reviriego, F., Navarro, P., García-España, E., Abelda, M. T., Frías, J. C., Domenech, A., Yunta, M. J. R., Costa, R. and Ortí, E. (2008). Diazatetraester ^1H-pyrazole crowns as fluorescent chemosensors for AMPH, METH, MDMA (ecstasy), and dopamine. *Organic Letters* **10**, 5099–5102.

Sánchez-Moreno, M., Marín, C., Navarro, P., Lamarque, L., García-España, E., Miranda, C., Huertas, O., Olmo, F., Gómez-Contreras, F., Pitarch, J. and Arrebola, F. (2012*a*). *In vitro* and *in vivo* trypanosomicidal activity of pyrazole-containing macrocyclic and macrobicyclic polyamines: their action on acute and chronic phases of Chagas disease. *Journal of Medicinal Chemistry* **55**, 4231–4243.

Sánchez-Moreno, M., Gómez-Contreras, F., Navarro, P., Marín, C., Olmo, F., Yunta, M. J. R., Sanz, A. M., Rosales, M. J., Cano, C. and Campayo, L. (2012*b*). Phthalazine derivatives containing imidazole rings behave as Fe-SOD inhibitors and show remarkable anti-*T. cruzi* activity in immunodeficient-mouse mode of infection. *Journal of Medicinal Chemistry* **55**, 9900–9913.

Stallings, W. C., Metzger, A. L., Pattridge, K. A., Fee, J. A. and Ludwig, M. L. (1991). Structure–function relationships in iron and manganese superoxide dismutases. *Free Radical Research Communications* **12–13**, 259–268.

Sundar, S. and Chatterjee, M. (2006). Visceral leishmaniasis: current therapeutic modalities. *Indian Journal of Medical Research* **123**, 345–352.

Turrens, J. F. (2004). Oxidative stress and antioxidant defences: a target for the treatment of diseases caused by parasitic protozoa. *Molecular Aspects of Medicine* **25**, 211–220.

Van Assche, T., Deschacht, M., Inocencio da Luz, R. A., Maes, L. and Cos, P. (2011). *Leismania*-macrophage interactions: insights into the redox biology. *Free Radical Biology and Medicine* **51**, 337–351.

World Health Organization (2010). *Expert Committee on the Control of Leishmaniases Meeting*. WHO Technical Reports Series No. 949. World Health Organization, Geneva, Switzerland.

Woster, P. M. (2007). Antiprotozoal agents (African trypanosomiasis, Chagas disease and leishmaniasis). In *Comprehensive Medicinal Chemistry II* (ed. Taylor, J. B. and Triggle, D. J.), pp. 815–842. Elsevier, Amsterdam, the Netherlands.

Yikilmaz, E., Xie, J., Brunold, T. C. and Miller, A. F. (2002). Hydrogen-bond-mediated tuning of the redox potential of the non-heme Fe site of superoxide dismutase. *Journal of the American Chemical Society* **124**, 3482–3483.

Yikilmaz, E., Rodgers, D. W. and Miller, A. F. (2006). The crucial importance of chemistry in the structure-function link: manipulating hydrogen bonding in iron-containing superoxide dismutase. *Biochemistry* **45**, 1151–1161.